

# A Triangular-shaped Quarter-mode Substrate Integrated Waveguide based Antenna for WBAN Applications

Divya Chaturvedi\* and S. Raghavan

Department of Electronics and Communication Engineering, National Institute of Technology, Tiruchirappalli - 620 015, India  
\*E-mail: divyanitt31@gmail.com

## ABSTRACT

In this study, a compact quarter-mode substrate integrated waveguide (QMSIW) based dual-band antenna is proposed for wireless body area network applications. A QMSIW resonator is realised by splitting the full-mode substrate integrated waveguide cavity along the perfect magnetic conductor walls. The proposed antenna preserves the fundamental mode  $TE_{110}$  and the third order mode  $TE_{220}$  of the square SIW cavity. The proposed antenna is linearly polarised in the lower band at 2.45 GHz and circularly polarised in the higher frequency band at 5.8 GHz. The on-body performance of the antenna is validated on a piece of pork muscle tissue and it has been found to be stable with respect to surroundings. The proposed antenna covers the ISM bands 44 MHz (2.445 GHz - 2.489 GHz) and 225 MHz (5.730 GHz - 5.955 GHz) at 2.45 GHz and 5.8 GHz, respectively. The measured gain of the antenna on pork tissue is 1.87 dBi and 5.5 dBi at two bands. In addition, the specific absorption rate is obtained of 0.65 mW/g and 1.51 mW/g at two bands ( $w_{\text{eff}} = 2$  mm), averaged over 1 g of muscle with 100mW input power. Moreover, the simulated and experimental results demonstrate a good agreement.

**Keywords:** Circularly polarised antenna; Off-body communication; Quarter mode substrate integrated waveguide; Wireless body area network

## 1. INTRODUCTION

For the past few years, wireless body area network (WBAN) has become a vital area of research in health monitoring applications, faster rescue operations, and data telemetry services. A great reduction in the cost of society, as well as comfort in treatment, is easily possible by remote telemetry. Based on its applications and the communication links, WBAN can be categorised as in-, on-, off-body communications<sup>1</sup>. For on-body communication, low profile compact size antennas are required to provide monopole-like radiation characteristics along the body surface<sup>2-3</sup>. For off-body communication the radiation pattern of the antenna required to be perpendicular to the surface of the wearer<sup>4-6</sup>. Back radiations and poor isolation from the body are big limitations in conventional types of antennas. A technique was proposed to minimise back radiations with the loading of CRLH transmission line<sup>7</sup> and inserting an insulated slab of high permittivity material<sup>8</sup>.

Recently, a keen interest in substrate integrated waveguide (SIW) technology has been ascribed to its important features of lower losses, high power handling capability, compact size, and good isolation from the surrounding medium due to its closed cavity structure<sup>9-10</sup>. SIW is a planar version of the waveguide which offers the advantage of the easy integration owing to its single-layer structure<sup>11</sup>. By using half-mode topology, the size of the cavity can be reduced up to half of the conventional cavity<sup>12,13</sup>. Further miniaturisation is possible by bisecting the half-mode SIW along one of the perfect magnetic wall. By

using quarter-mode substrate integrated waveguide (QMSIW) topology, the size is reduced up to  $1/4^{\text{th}}$  of the conventional cavity by maintaining the comparable performance<sup>14-17</sup>.

On the other hand, WBAN demands the circularly polarised antennas to eliminate the problem of multipath interference. Some circularly polarised microstrip patch antennas have been introduced<sup>18-19</sup> by exciting the orthogonal modes with a  $90^\circ$  phase difference. The different class of circularly polarised antennas based on QMSIW resonator<sup>20-21</sup> have been considered better options because they offer high performance in a compact structure. Multi-band antennas are always preferred because they can perform a number of operation at the same time. A dual-band on-body repeater antenna was introduced for on-body communication<sup>22</sup>. To offer the flexibility in structure, SIW cavity-backed antennas are fabricated using textile materials, which facilitate conformity on discontinuous surfaces<sup>23</sup> and can be directly integrated into the garments.

A compact dual-band antenna is proposed to operate at 2.45 GHz and 5.8 GHz covering the ISM bands of (2.4 GHz - 2.5 GHz) and (5.725 GHz - 5.875 GHz) for WBAN applications. The miniaturisation is achieved by deploying advantage of symmetric E-field distribution along the perfect magnetic walls, hence the size is diminished up to  $1/4^{\text{th}}$  of conventional square SIW structure<sup>8</sup>. The proposed antenna contains the advantages of compact size, simple geometry, single-layered structure, along with it preserved the cavity features. In spite of the two open side walls, the performance of the antenna is minimally sensitive to the surroundings, which reveals that the proposed geometry is a suitable option for off-body communication<sup>10</sup>.

2. ANTENNA DESIGN METHODOLOGY

2.1 Design Evolution

The resonant frequency for square SIW cavity can be calculated from the Eqn (1)<sup>15</sup>

$$f_r(TE_{110}) = \frac{c}{2\sqrt{\epsilon_r}} \sqrt{\left(\frac{1}{W}\right)^2 + \left(\frac{1}{L}\right)^2} \quad (1)$$

$L$  is the length of the cavity,  $W$  is the width of the cavity,  $c$  is the velocity of light in free space,  $\epsilon_r$  is the relative permittivity of the substrate.

When the square SIW cavity is cut along the quasi-fictitious magnetic wall  $A-A'$ , half mode field distribution of mode  $TE_{110}$  and  $TE_{220}$  is realised. Hence, by using this technique 50 per cent size of the cavity is reduced by preserving the half-modes of  $TE_{110}$  and  $TE_{220}$  of the square SIW cavity<sup>13-15</sup>. In a similar way QMSIW can be realised, if HMSIW cavity is again bisected along the magnetic wall  $O-B$ , hence 75 per cent size reduction is attained than FMSIW cavity<sup>15</sup>, as shown in Fig. 1(b)

2.2 Full-Mode Substrate Integrated Waveguide

Figures 2(a) and 2(b) E-field distribution of FMSIW cavity is displayed for  $TE_{110}$  mode at 3.2 GHz and  $TE_{220}$  mode at 6.04 GHz. These two modes are involved for designing the antenna to cover the ISM bands at 2.45 GHz and 5.8 GHz.

2.3 Quarter-Mode Substrate Integrated Waveguide

To attain the QMSIW, the half-mode SIW cavity is bisected along the wall  $O-B$ , shown in Fig. 1(b). The dominant mode  $TE_{110}$  and third order mode  $TE_{220}$  are preserved in a QMSIW cavity due to its symmetrical field distribution along the magnetic walls. E-field distribution of QMSIW has been shown in Figs. 3(a), 3(b), and 3(c).

Three different resonant frequencies are characterised by two different modes. First resonance is observed at 2.45 GHz due to the  $TE_{110}$  mode while second and third resonances

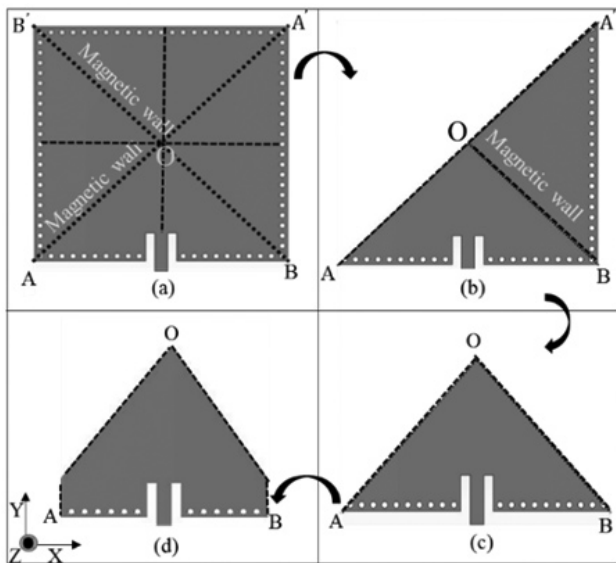


Figure 1. Design evolution: Miniaturisation process from FMSIW to QMSIW (a) FMSIW (b) HMSIW (c) QMSIW (d) and Proposed antenna.

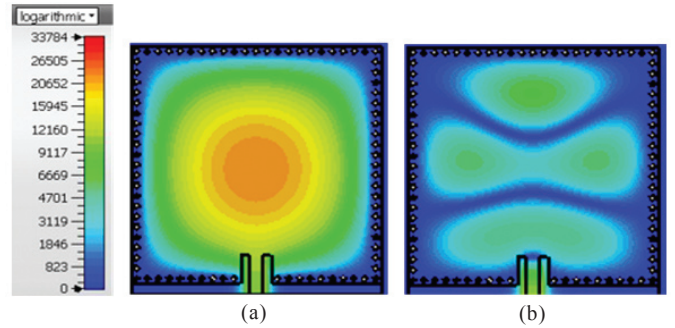


Figure 2. E-field distribution in FMSIW (a)  $TE_{110}$  mode at 3.2 GHz (b)  $TE_{220}$  at 6.04 GHz.

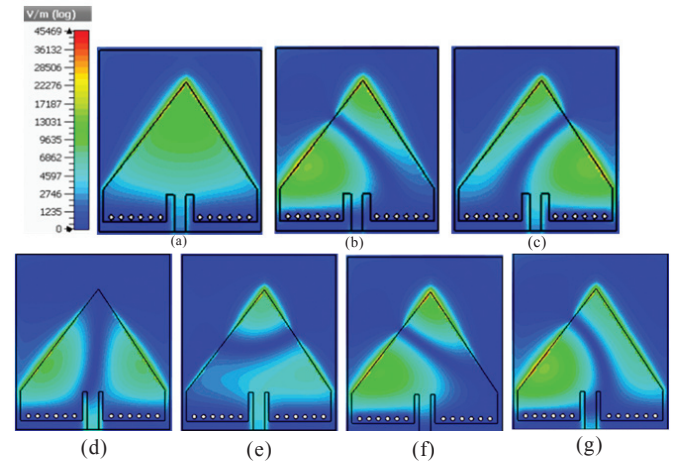


Figure 3. E-field distribution in QMSIW (a)  $TE_{110}$  at 2.45 GHz, (b)  $TE_{220}$  at 5.8 GHz, (c)  $TE_{220}$  at 5.8 GHz, distribution of E-field at 5.89 GHz, (d) phase =  $0^\circ$  (e) phase =  $45^\circ$  (f) phase =  $90^\circ$  (g) phase =  $135^\circ$ .

are observed at 5.8 GHz and at 5.89 GHz, due to mode  $TE_{220}$ , shown in Fig. 4. The bandwidth is enhanced in higher band due to excitation of two orthogonal degenerate modes of  $TE_{220}$ . From Figs. 3(b) and 3(c), shows the E-field distribution of orthogonal modes at 5.8 GHz and 5.89 GHz<sup>19</sup>. The electric field distribution of orthogonal modes can be made equal by tuning the length  $l_1$  and  $l_2$  of the dielectric aperture edges. By keeping a slight difference in the lengths of the edges, two orthogonal modes are getting excited close to each other with a phase difference of  $90^\circ$ , resulting in a circular polarisation is achieved in the far field region. The magnitude of E-field distribution has been shown at the phase of  $0^\circ$ ,  $45^\circ$ ,  $90^\circ$ ,  $135^\circ$  in the Figs. 3(d), 3(e), 3(f), and 3(g).

2.4 Proposed Antenna Geometry

The proposed antenna is designed on single-layered RT Duroid 5880 substrate of thickness 0.787 mm, the dielectric constant of 2.2 and loss tangent of 0.0009, as shown in Fig. (5). The size of the proposed antenna is 37 mm  $\times$  32 mm excited through the microstrip feeding technique, which offers the advantage of radiating parts on the single side of the cavity. All the simulation studies are carried out using CST microwave studio simulation solver.

Dimensions of the antenna are defined in (mm)  $L = 37$ ,  $W = 32$ ,  $l_1 = 27.8$ ,  $l_2 = 26.4$ ,  $l_3 = 6.5$ ,  $d_{\text{offset}} = 9.5$ ,  $d_{\text{via}} = 1$ ,  $s_{\text{via}} = 2$ ,  $d_1 = 1.4$ ,  $d_2 = 5.8$ ,  $w_{\text{ext}} = 0.8$ ,  $w_f = 2.5$ .

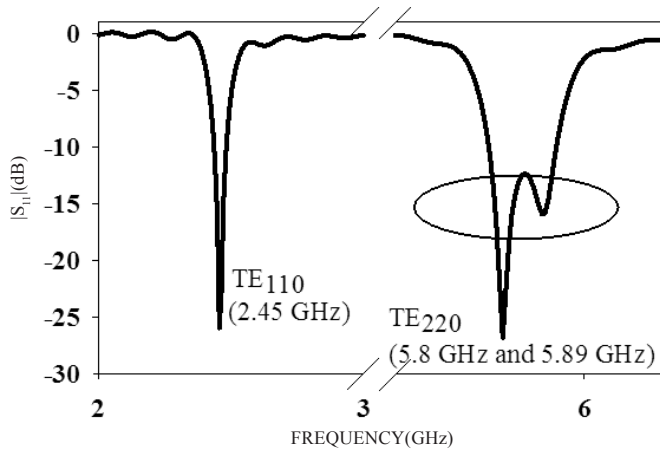


Figure 4. Reflection coefficient with frequency of proposed antenna.

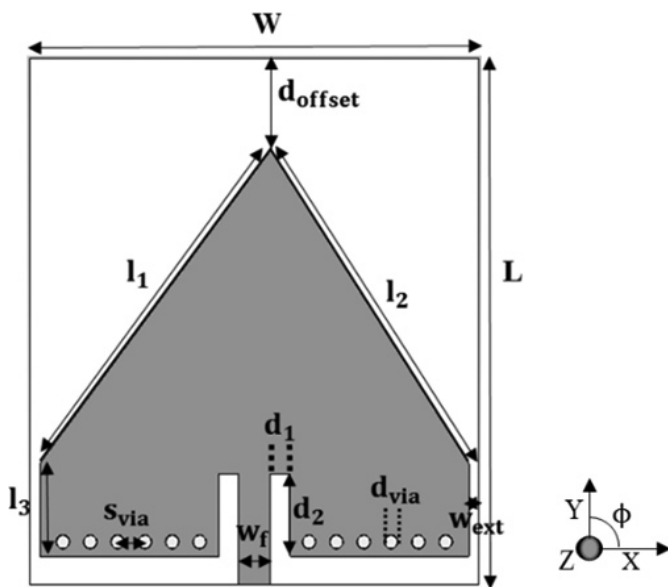


Figure 5. Configuration of proposed QMSIW antenna.

### 3. PARAMETRIC ANALYSIS

#### 3.1 Investigation of Parameters in Free Space

Figure 6, the reflection coefficients with frequency is plotted by changing the position of  $C_t$  from the center point towards +ve X-axis, which creates a difference in the lengths of the open edges of the cavity and changes the electric field distribution. Since, the lower band shows insignificant variation compared to higher band with respect to  $C_t$ , hence parametric analysis has been shown in Fig. 6 only for the higher band. The splitting of both the degenerate modes mainly depends upon the difference between the edges of the cavity, hence bandwidth is enhance by shifting the position of  $C_t$  towards the right side. Maximum bandwidth up to 185 MHz is achieved with the optimised value of  $C_t = 1.6$  mm.

The ground plane size is an important parameter to maintain the stable on-body performance of the proposed antenna. There is always a trade-off between the size and performance of the antenna. The effect of the ground plane size on impedance characteristic of the higher band has been shown

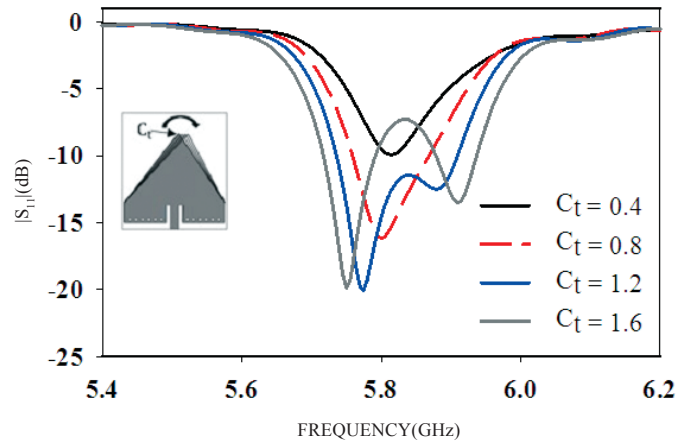


Figure 6. Reflection coefficient with frequency for different  $C_t$  values.

in Fig. 7. By extending the dimensions of the ground plane, impedance bandwidth increases slightly as well as impedance matching improves significantly in a higher band.

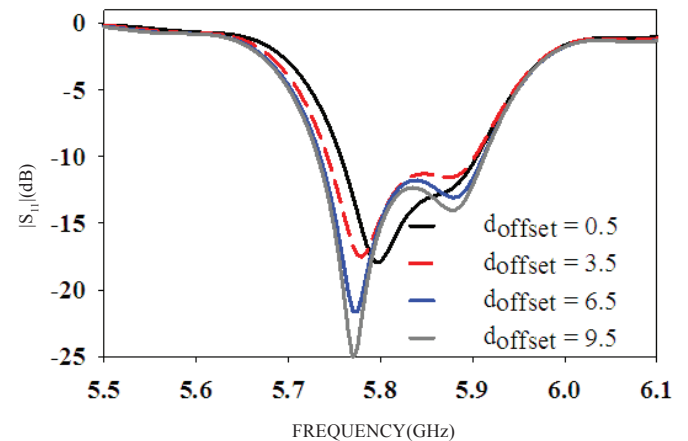


Figure 7. Reflection coefficient with frequency for different  $d_{offset}$  values.

#### 3.2 Investigation of Parameters on Pork Muscle Tissue

Figure 8 illustrates the reflection coefficient plots with frequency in free space and in proximity of the phantom. It has been noticed that frequency shifts up slightly in presence of the phantom. Anyway, variation in bandwidth is nominal in all of the cases. The proposed antenna shows stable performance both in free space and on the pork muscle equivalent phantom.

Figure 9, parametric studies are performed in bent condition on the cylindrical phantom of the radius of curvature 30 mm and 60 mm as well as in flat condition on the large rectangular phantom of dimensions 200 mm × 180 mm × 50 mm. The cylindrical phantom is considered as equivalent to the human arm<sup>5,11</sup>. The reflection coefficient from the realistic Emma body model<sup>24</sup>, which is available in CST Microwave Studio solver shows the almost similar performance of muscle equivalent phantom. A significant deviation has been observed, when the antenna is bent on the cylindrical phantom of smaller radius of curvature ( $r = 30$  mm). This happens due to increase

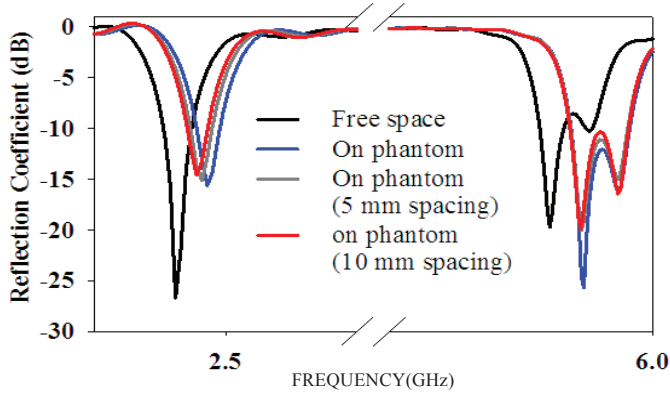


Figure 8. Reflection coefficients against frequency with different spacing of pork muscle phantom.

in the bending effect and decreases in the tolerance.

A rectangular flat phantom is considered as equivalent to 2/3 of permittivity and conductivity of pork muscle tissue<sup>5,15</sup> and the properties of the phantom are  $\epsilon_r$  35.8 and  $\sigma$  1.2 S/m at 2.45 GHz and  $\epsilon_r$  32.3 and  $\sigma$  3.5 S/m at 5.8 GHz<sup>24</sup>. In order to verify the on-phantom simulation results, the antenna is tested on pork muscle tissue<sup>5</sup>, as shown in Fig. 10 and measurements are performed with Agilent E5071B (ENA) series Network Analyser. The permittivity and conductivity of the tissue are measured as  $\epsilon_r$  34.5 and  $\sigma$  0.7 S/m at 2.45 GHz and  $\epsilon_r$  31.6 and  $\sigma$  2.7 S/m at 5.8 GHz. A good agreement between the numerical phantom and pork muscle tissue confirms that the pork tissue is a good substitution of the human body.

Table 1. Comparison of parameters in free space and on pork muscle tissue

Parameters		Lower band		Upper band	
		Free space	On pork	Free space	On pork
$f_0$ (GHz)	Sim.	2.456	2.478	5.78	5.81
	Meas.	2.46	2.48	5.79	5.815
BW (MHz)	Sim.	51	45	179	162
	Meas.	48	44	184	225
Gain (dBi)	Sim.	2.64	1.95	5.5	5.8
	Meas.	2.2	1.87	5.35	5.5
Efficiency	Sim.	55%	38%	78%	69%

The measured reflection coefficient plot on pork muscle tissue shows the -10 dB impedance bandwidth of 44 MHz (2.445 GHz - 2.489 GHz) in the lower frequency band and 225 MHz (5.730 GHz - 5.955 GHz) in the higher frequency band. The reflection coefficient plots exhibit that the simulated and measured results on pork muscle are close to each other. Figure 12(a) illustrates simulated and measured gain in free space and axial ratio plots with respect to frequency. The simulated 3dB axial ratio bandwidth is 98 MHz (5.746 GHz - 5.844 GHz) and the measured bandwidth is 52 MHz (5.776 GHz - 5.828 GHz) at 5.8 GHz on pork. The simulated peak gains are 1.95 dBi and 5.8 dBic for the lower and the higher band on phantom. Figure 12(b) illustrates variation of SAR with frequency over 1 g mass of tissues at two bands 2.45 GHz and 5.8 GHz, respectively.

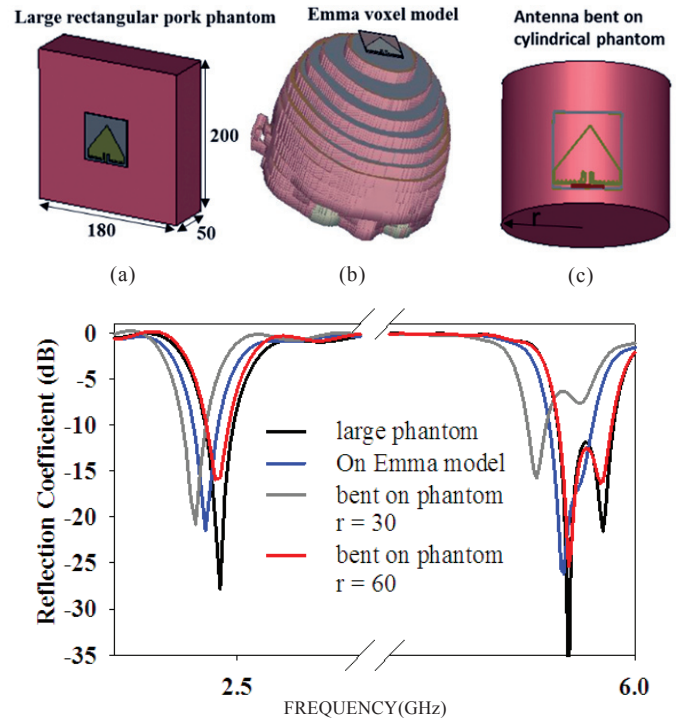


Figure 9. Reflection coefficient variation with frequency (a) on large rectangular phantom (b) on Emma voxel model (c) bent on cylindrical pork phantom.

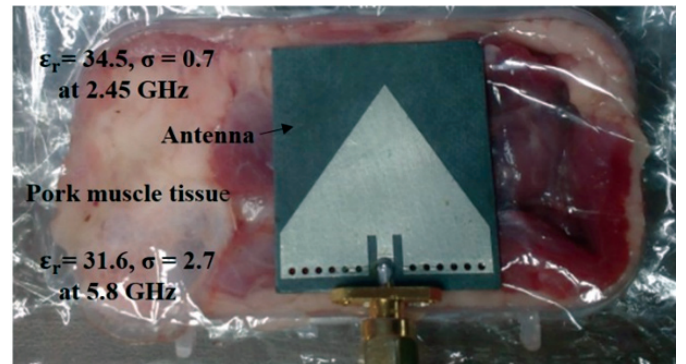


Figure 10. Measurement setup on pork muscle tissue.

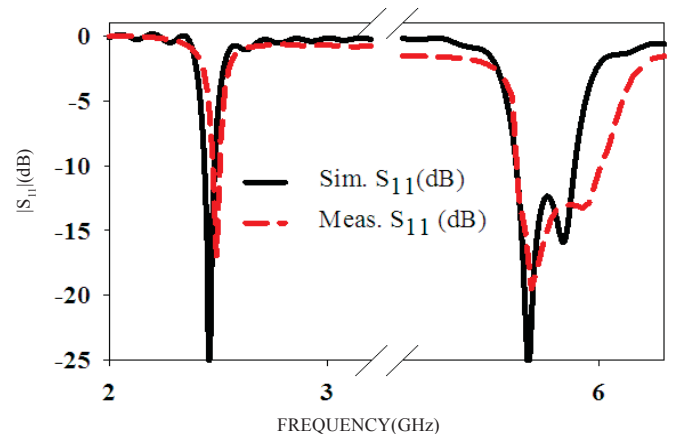


Figure 11. Comparison of simulated and measured reflection coefficient plots with frequency on pork muscle.

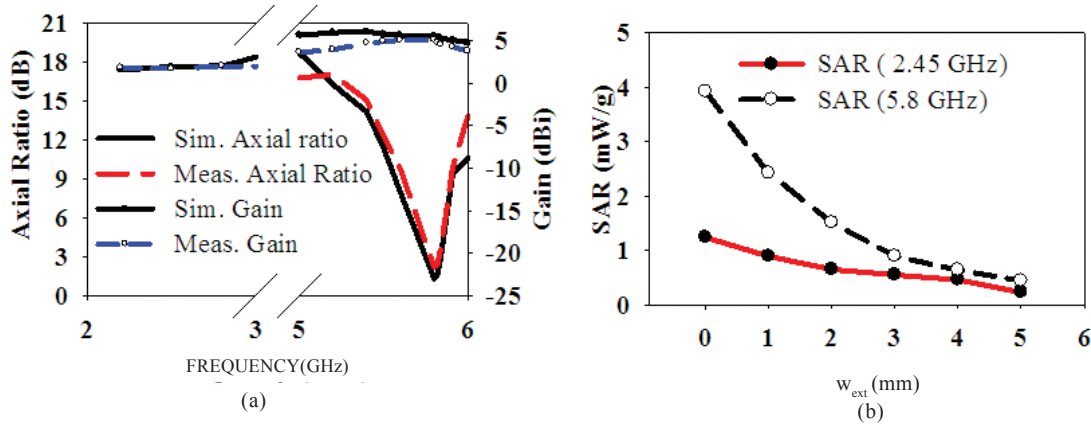


Figure 12. (a) Simulated and measured axial ratio plot with frequency on phantom (b) SAR plots with frequency.

Figures 13 (a)-13(b) show the linearly co-polarised and cross polarised radiation pattern plots for the lower band at H-plane ( $\phi = 0^\circ$ ) and E-plane ( $\phi = 90^\circ$ ). It can be observed from both of the plots that maximum radiation is oriented towards the boresight direction with a peak gain of 1.87 dBi. Figure 13(c)-13(d) show the co-polarised (RHCP) and cross polarised (LHCP) radiation pattern plots at 5.8 GHz at H-plane ( $\phi = 0^\circ$ ) and E-plane ( $\phi = 90^\circ$ ). The proposed antenna shows maximum co-polarised RHCP gain of 5.5 dBi in direction  $\theta = 45^\circ$ . At 5.8 GHz simulated peak gain value on a phantom is noticed to be higher than in free space because of significant decrease in the back radiations and cross-polarisation due to presence of lossy phantom. The cross-polarised radiations are 15 dB lower than co-polarised radiations at 2.45 GHz, which shows a good polarisation purity. The proposed antenna has advantages of compact simple geometry, dual band operations, and single feed circular polarisation. The microstrip feed is always desirable in body worn applications because of its planar nature as well as it maintains the integrity of ground plane. The proposed antenna provides the robust performance on pork tissue in terms of frequency detuning, impedance matching, and radiation characteristics. In Table 2, characteristic parameters are compared with existing antennas and it has been observed that the proposed antenna has lower efficiency than other designs, but anyway it is sufficient for WBAN applications.

4. CONCLUSIONS

A quarter-mode SIW antenna is proposed for WBAN applications in this paper. The size of the proposed antenna is reduced by 75 per cent with the concept of quarter-mode

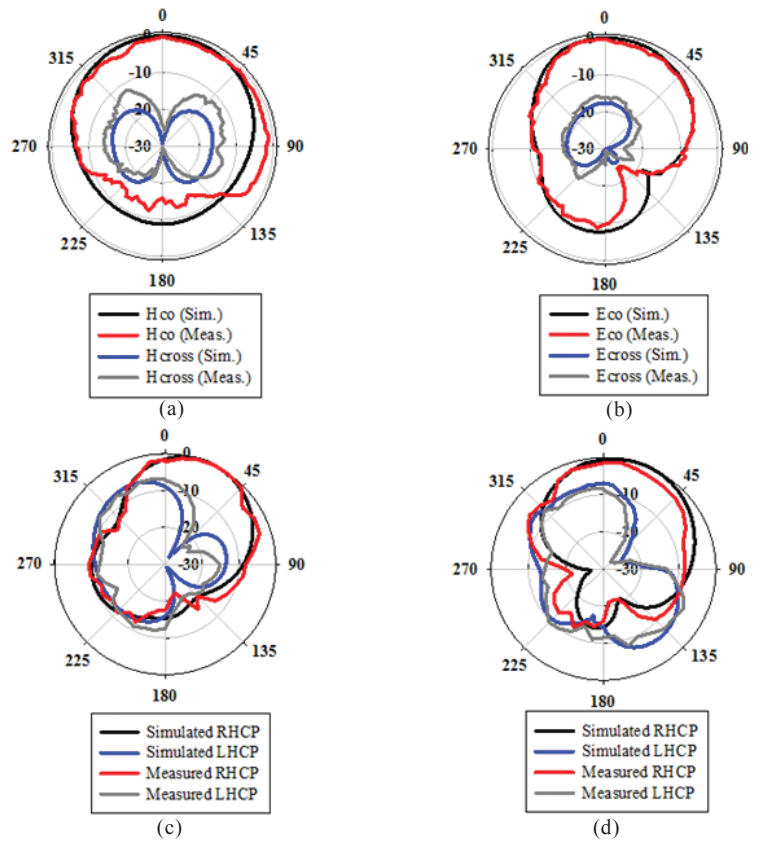


Figure 13. Simulated and measured radiation pattern plots on pork phantom co-pol. (black solid line), Measured co-pol. (red solid line), simulated cross pol. (Blue solid), measured cross pol. (Grey solid) (a), (b) E-plane ( $\phi = 90^\circ$ ), H-plane ( $\phi = 0^\circ$ ) at 2.45 GHz (c), (d) ( $\phi = 0^\circ$ ) and ( $\phi = 90^\circ$ ) at 5.8 GHz.

Table 2. Comparison with previous research studies

Ref.	Antenna Size (mm <sup>2</sup> )	Frequency band (GHz)	Bandwidth (MHz)	Substrate	Thickness (mm)	$\epsilon_r$	Gain (dBi)	Sim. Effi. (per cent)
ZG & Guo <sup>4</sup>	5728	2.4, 5.8	85/200	RT 5870	1.6	2.33	0.75/5.4	NA
Zhu <sup>5</sup> , et al.	986	2.4, 5.8	30/114	RT 5870	1.6	2.33	2.13/5.16	60/76
Tahir & Javed <sup>6</sup>	1175	2.4, 5.2	140/160	Denim	1	1.68	3.1/3.5	NA
Agnessens & Rogier <sup>13</sup>	3985	2.4, 5.8	80/150	Rubber protective foam	3.94	1.49	4.4/5.7	72.8/88
Proposed work	1184	2.45, 5.8	44/225	RT 5880	0.8	2.2	1.87/5.5	38/69

SIW topology and similar performance of FMSIW cavity is maintained. Shorted vias cavity type structure and complete ground plane facilitate good isolation from the body. The proposed antenna shows robust performance in the on-body stringent conditions with moderate gain and unidirectional radiation pattern. All the performance parameters confirm that the proposed antenna can be optimally utilised for off-body communication.

## REFERENCES

- Pellegrini, A.; Brizzi, A.; Zhang, L.; Ali, K.; Hao, Y.; Wu, X.; X., Constantinou, C. C.; Nechayev, Y.; Hall, P. S.; Chahat, N.; Zhadobov, M. & Sauleau, R. Antennas and propagation for body-centric wireless communications at millimeter wave frequencies: A review. *IEEE Antennas Propag. Mag.*, 2013, **55**(4), 262–87. doi: 10.1109/MAP.2013.6645205
- Kang, D.G.; Tak, J. & Choi, J. Low-profile dipole antenna with parasitic elements for WBAN applications. *Microw. Opt. Technol. Lett.*, 2016, **58**(5), 1093–97. doi: 10.1002/mop.29749
- Ma, D. & Zhang, W.X. Coupling-fed circular-patch antenna for on-body communication system. *Microw Opt. Technol. Lett.*, 2009, **51**(11), 2623–27. doi: 10.1002/mop.24712
- ZG, L. & Guo, Y.X. Dual band low profile antenna for body centric communications. *IEEE Trans. Antennas Propag.*, 2013, **61**(4), 2282–85. doi: 10.1109/TAP.2012.2234071
- Zhu, X.Q.; Guo, Y.X. & Wen, W. A compact dual-band antenna for wireless body-area network applications. *IEEE Antennas Wirel. Propag. Lett.*, 2016, **15**, 98–01. doi: 10.1109/LAWP.2015.2431822
- Tahir, F.A. & Javed, A. A compact dual-band frequency-reconfigurable textile antenna for wearable applications. *Microw. Opt. Technol. Lett.*, 2015, **57**(10), 2251–57. doi: 10.1002/mop.29311
- Yan, S.; Soh, P.J. & Vandenbosch, G.A.E. Compact all-textile dual-band antenna loaded with metamaterial-inspired structure. *IEEE Antennas Wirel. Propag. Lett.*, 2015, **14**, 1486–89. doi: 10.1109/LAWP.2014.2370254
- Aslam, B.; Khan, U.H.; Muhammad, A.A.; Amin, Y.; Loo, J. & Tenhunen, H. Miniaturized decoupled slotted patch RFID tag antennas for wearable health care. *Int. J. RF Microw. CAD Eng.*, 2016, **27**(1). doi: 10.1002/mmce.21048
- Luo, G.Q.; Hu, Z.F.; Dong, L.X. & Sun, L.L. Planar slot antenna backed by substrate integrated waveguide cavity. *IEEE Antennas Wirel. Propag. Lett.*, 2008; **7**, 236-9. doi: 10.1109/LAWP.2008.923023
- Khan, A.A. & Mandal, M.K. Miniaturized substrate integrated waveguide (SIW) power dividers. *IEEE Microw. Wirel. Compon. Lett.*, 2016, **26**, 888-90. doi: 10.1109/LMWC.2016.2615005
- Hong, Y.; Tak, J. & Choi, J. An all-textile SIW cavity-backed circular ring-slot antenna for WBAN applications. *IEEE Antennas Wirel. Propag. Lett.*, 2016, **15**, 1995–99. doi: 10.1109/LAWP.2016.2549578
- Razavi, S.A. & Neshati, M.H. Development of a linearly polarized cavity-backed antenna using HMSIW technique. *IEEE Antennas Wirel. Propag. Lett.*, 2012, **11**, 1307-10 doi: 10.1109/LAWP.2012.2227231
- Agneessens, S. & Rogier, H. Compact half diamond dual-band textile HMSIW on body antenna, *IEEE Trans. Antennas Propag.*, 2014, **62**, 2374–81. doi: 10.1109/TAP.2014.2308526
- Agneessens, S.; Lemey, S.; Vervust, T. & Rogier, H. Wearable, small, and robust: The circular quarter-mode textile antenna. *IEEE Antennas Wirel Propag. Lett.*, 2015,**14**, 1482–85. doi:10.1109/LAWP.2015.2389630
- Chaturvedi, D. & Raghavan, S. Circular quarter-mode SIW antenna for WBAN application. *IETE J Res.* 2017, 1-7. doi:10.1080/03772063.2017.1358115
- Banerjee, S.; Roy, K.; Mohanty, T.; Ray, S.; Sarkar, T. S. & Gangopadhyaya, M. Quarter-mode SIW based compact triangular antenna for 2.5 GHz cellular spectrum. In Ubiquitous Computing, Electronics & Mobile Communication Conference (UEMCON), IEEE Annual, 2016, 1-4. doi:10.1109/UEMCON.2016.7777843
- Wang, T.; Fang, S. & Zhu, S. A novel miniaturized quarter-mode circular polarization antenna based on SIW loaded with dual-CSR for BDS application. In Asia-Pacific Microwave conference (APMC) 2014, 1402-04. ISBN: 978-1-4799-6055-2
- Sharma, P. & Gupta, K. Analysis and optimized design of single feed circularly polarized microstrip antennas. *IEEE Trans. Antennas Propag.*, 1983, **31**(6), 949–955. doi: 10.1109/TAP.1983.1143162
- Shahabadi, M.; Busuioc, D.; Borji, A. & Safavi-Naeini, S. Low-cost,high-efficiency quasi-planar array of waveguide-fed circularly polarized microstrip antennas. *IEEE Trans. Antennas Propag.*, 2005, **53**(6), 2036 – 43.
- Jin, C.; Li, R.; Alphones, A. & Bao, X. Quarter-mode substrate integrated waveguide and its application to antennas design. *IEEE Trans. Antennas Propag.*, 2013, **61**(6), 2921–28. doi: 10.1109/TAP.2013.2250238
- Kyeoungseob, K.; & Sungjoon, L. Miniaturized circular polarized TE<sub>10</sub> -mode substrate-integrated-waveguide antenna. *Ant. Wirel. Propag. Lett.*, 2014, **13**, 658-661. doi: 10.1109/LAWP.2014.2313747
- Tak, J.; Kwon, K.; Kim, S. & Choi, J. Dual-band on-body repeater antenna for in-on-on WBAN applications. *Int. J. Antennas Propag.*, **2013** (2013). doi: 10.1155/2013/107251
- Moro, R.; Agneessens, S.; Rogier, H. & Bozzi, M. Wearable textile antenna in substrate integrated waveguide technology. *Electron. Lett.*, 2012, **48**(16), 985–87. doi: 10.1049/el.2012.2349
- Dielectric properties of human body. <http://niremf.ifac.cnr.it/tissprop/>. (Accessed on 10 June 2017).

## CONTRIBUTORS

**Ms Divya Chaturvedi** received her BTech (Electronics and Communication Engineering) from Uttar Pradesh Technical University, India and MTech (Electronics Engineering) from Pondicherry Central University, India. Currently pursuing her PhD at National Institute of Technology, Tiruchirappalli. Her area of research involves : Substrate integrated waveguide, microwave integrated circuits, metamaterial and biological effects of radiation on human body.

In this study, he has proposed an substrate integrated waveguide antenna for off-body communication applications at 2.4 Ghz and 5.8 GHz. The proposed design is compact, single-layered, robust, offers high performance in proximity to the lossy body tissues.

**Dr S. Raghavan** received his BE (ECE) from College of Engineering, Guindy, and ME (Microwave Engineering) from College of Engineering, Trivandrum. He received his PhD from IIT Delhi, India. Currently working as Senior Professor at National Institute of Technology, Tiruchirappalli, India. His research interest includes : Microwave/millimeter-wave circuits and devices, microwave integrated circuits, antennas, EMI/EMC, computational Electromagnetics, RF/BIO MEMS, Metamaterials and microwaves in biomedical applications. He has contributed more than 100 papers in journals and 200 papers in conferences proceedings.

Contribution in the current study he has analysed the antenna in free space and in proximity to the pork tissues, which shows a stable performance, and confirms that the proposed geometry is suitable option for off-body communication.